Downscaling an eddy-resolving global ocean model for the continental shelf off southeast Australia.

Mark E. Baird [a,*] Helen S. Macdonald [a] Moninya Roughan [a,b]
Peter R. Oke [c]

[a] *Coastal and Regional Oceanography Laboratory, School of Mathematics and Statistics, University of NSW, Sydney NSW, 2052, Australia*

[b] *Sydney Institute of Marine Science, Mosman, NSW, 2088, Australia*

[c] *CSIRO Marine and Atmospheric Research and Wealth from Oceans Flagship Program, Hobart, Tasmania, Australia*

Abstract

An eddy-resolving global ocean model (BRAN) is downscaled for the waters off southeast Australia and the performance assessed against remotely-sensed and shipboard observations. The downscaling involves assimilating hydrographic fields from a ∼10 km resolution global analysis (BODAS) into a ∼3 km resolution southeast Australian configuration of the Princeton Ocean Model (SEAPOM). Numerical experiments establish that the optimal strength and duration of the assimilation of BODAS fields into the SEAPOM configuration for the purpose of producing hindcasts of ocean state is 1 d^{-1} for 1 day. SEAPOM, BRAN and BODAS are assessed against two high resolution SST products for the austral summer and winters of 2002-2006. SEAPOM achieves best results in winter when the remote forcing is weakest, obtaining a root mean square error of 1.01°C on the continental shelf, reducing the errors relative to BRAN by ∼0.12°C. For the whole domain extending ∼400 km offshore, the improvement in winter is ∼0.03°C. In summer when temperature variability is the greatest, SEAPOM has a similar performance to BRAN both on and off the shelf. A more detailed comparison is made against vertical slices of temperature and velocity obtained *in situ* using a towed SeaSoar in September 2004. This comparison shows the higher resolution SEAPOM configuration resolves frontal features better than the coarser BRAN. The downscaling effort improves the estimation of ocean state off southeast Australia, especially on the continental shelf, in winter, and for finer spatial features.

Key words: East Australian Current, data assimilation, model initialisation, Bluelink, Princeton Ocean Model

1 Introduction

The continental shelf off southeast Australia varies in width from a minimum of 16 km off Smoky Cape (31°S) to a maximum of ∼50 km off Newcastle (33°S) (Fig. 1). The processes on the continental shelf are dominated by the presence of the East Australian Current (EAC), a strong poleward-flowing western boundary current, and the mesoscale eddies that are spawned at its separation (Cresswell and Legeckis, 1986; Tilburg et al., 2001; Ridgway and Dunn, 2003). In particular, the interaction between the uplift of slope water due to the bottom stress associated with the EAC and the alongshore wind stress drives intermittent upwelling along the southeast Australian coast (Oke and Middleton, 2001; Roughan and Middleton, 2002).

Understanding the continental shelf circulation off southeast Australia is important, among other reasons, because of: (1) the role of filaments of upwelled water in determining the carbon (Macdonald et al., 2009) and nitrogen (Baird et al., 2006b) shelf budgets, and the population dynamics of algal blooms (Ajani et al., 2001); (2) the dispersal of marine populations from coastal sites (Booth et al., 2007; Banks et al., 2007; Roughan et al., in prep.); (3) the need for effective positioning of marine parks (NSW Marine Parks Authority, 2008); (4) and locally important issues such as the presence of large discharges of treated sewerage (Pritchard et al., 1997) and de-salination brine (Sydney Water, 2005) off Sydney. Each of these phenomenon depend on processes that occur on spatial scales of less than 10 km. In particular, the baroclinic radius of deformation that approximates the seaward extent of the surfacing of wind-driven upwelling plumes is approximately 5-8 km in the region (Roughan and Middleton, 2002).

A coarse ∼10 km regional configuration of the Princeton Ocean Model (POM)

* Corresponding author.
Email address: m.baird@unsw.edu.au (Mark E. Baird).

for the waters off southeast Australia has previously been used to investigate coastal upwelling (Oke and Middleton, 2001) and particle trajectories (Roughan et al., 2003), finding the importance in particular of bottom water transport. More recently a ∼3 km configuration for the waters off southeast Australia has been applied to consider details of the underwater light field (Baird et al., 2007) and biogeochemical processes (Macdonald et al., 2009). These numerical simulations have been necessarily idealised and short in duration due to strong inflows on the northern boundary and the importance of non-linear mesoscale processes whose dynamics have not been captured. In order to provide both more realistic and longer duration simulations, the regional model needs to exploit ocean state estimates to incorporate the effects of remote forcing, account for non-linear mesoscale processes, and to correct for model errors during model integration.

Recently the Bluelink Project, a partnership between CSIRO, the Bureau of Meteorology and the Royal Australian Navy, has greatly increased Australia's ocean modelling capabilities (for a list of acronyms used in this paper see Table. 1). This has resulted in BRAN (Bluelink ReANalysis), an ensemble optimal interpolation reanalysis system applied to a global ocean general circulation model with a 0.1° (∼10 km) spatial resolution around Australia (Oke et al., 2005, 2008). BRAN is presently available as a daily hindcast of ocean state from October 1992 and is likely to be provided on an on-going basis.

Products from the Bluelink project have been used to investigate the mesoscale dynamics of waters off southeast Australia. Oke et al. (2005, 2008) demonstrated good qualitative agreement between reanalysed sea-level and Lagrangian tracks of surface drifting buoys in the Tasman Sea. Schiller et al. (2008) showed that the EAC transport in BRAN2p1, including the barotropic component, is at the upper end of earlier estimates derived from observation-based transport estimates. One interesting result from this study was that in the retroflection zone, and along the Tasman Front, they found vertical velocities of up to ±20

m d^{-1}. BRAN has also been used to show the interaction of local and remote processes leading to three anomalous SST events in the Coral Sea (Schiller et al., 2009).

In the present 0.1° resolution BRAN configuration it is expected that a number of coastal and continental shelf processes may not be well resolved. In particular, the coastline itself is represented by pixels with ∼10 km edges, limiting the use of BRAN velocity fields for the purpose of studying particles released from or settling on, the complex coastline. Furthermore, the horizontally uniform thickness of vertical layers and the polar horizontal grid are not well suited to processes such as topographic steering, shelf break dynamics and bottom boundary layer transport. To capture the dynamics of coastal and continental shelf regions as influenced by remote and mesoscale processes requires an eddy-resolving global model to be downscaled to a shelf-scale model.

In this paper, the archived temperature and salinity fields of the Bluelink Ocean Data Assimilation System (BODAS) are assimilated into a ∼3 km resolution configuration of the Princeton Ocean Model for the waters off southeast Australia (SEAPOM). To optimise assimilation effectiveness, numerical experiments are undertaken to find the most suitable strength and duration of assimilation. Three month model simulations are then undertaken for the austral summer (December-February) and winter (June-August) for 2002-2006. For these 10 integrations, a comparison is undertaken of the analysed data (BODAS), the re-analysis (BRAN) and the downscaled model (SEAPOM) against independent SST observations. Finally, *in situ* observations from September 2004 are used to investigate the ability of the downscaled model to improve the representation of smaller scale processes.

2 Methods

The modelling system detailed in this paper involves assimilating data from a global analysis with ∼10 km resolution in the Australian region (BODAS) into a regional POM configuration with a ∼3 km resolution (SEAPOM). By assimilation, we refer to the relaxation of model state to the analysis, that might also be referred to as initialisation. SEAPOM output is compared with output from BRAN, a similar reanalysis product at the same resolution as the analysis. Each component of the modelling system is described in detail below.

2.1 BODAS

The data assimilation system developed under Bluelink is the Bluelink Ocean Data Assimilation System (BODAS; Oke et al. (2008)). BODAS employs an ensemble optimal interpolation (EnOI) scheme that uses a stationary, 120-member ensemble of intraseasonal model anomalies to approximate the system's background error covariance. The covariances that are implicit to the ensemble are used to interpolate and extrapolate observations onto the 0.1° resolution model grid. The system is multivariate, using observations of one type (e.g., temperature) to update fields of all types (temperature, salinity, velocity, and sea-level). BODAS was specifically developed for application to long reanalyses, like the Bluelink ReANalysis (BRAN; see below), and for operational short-range forecast system of the mesoscale ocean circulation around Australia. Consequently, computational efficiency was an important consideration in its development. As a result, BODAS employs practical "short-cuts" that make its implementation feasible for the intended applications. For a comprehensive description of BODAS, the reader is referred to Oke et al. (2008).

2.2 BRAN

BRAN is a multi-year model integration with sequential data assimilation. The Bluelink model is a global configuration of MOM4p0d (Griffies et al., 2004), with 0.1° resolution around Australia and coarser elsewhere. Version 2p1 of BRAN, hereafter BRAN2p1, used in this study, spans the period October 1992 to December 2006. For BRAN2p1 the model is forced with 6-hourly surface fluxes, provided by the European Center for Medium Range Weather Forecasting (ECMWF). Observations assimilated by BRAN include sea-level anomalies from along-track altimetry and coastal tide gauge stations, satellite SST from the AMSR-E mission and Pathfinder database, *in situ* temperature and salinity from the Argo program, and temperature from XBT sections and tropical moorings. Data are assimilated once a week. For each assimilation cycle, observations from a time window of up to 9 days is used. Observations collected before or after the analysis time are ascribed a larger observation error, to down-weight their influence on an analysis.

Oke et al. (2008) showed that in the region around Australia, fields from version 1p5 of BRAN (BRAN1p5), are typically within 6-12 cm of withheld altimetric observations, within 0.5-0.9°C of observed SST and within 4-7 cm of observed coastal sea-level. Comparisons with Argo profiles and surface drifting buoys show that BRAN fields are within 1°C of observed sub-surface temperature, within 0.15 of observed sub-surface salinity and within 0.2 m s^{-1} of near-surface currents. Results of BRAN2p1 are presented by Schiller et al. (2008), showing details of the seasonal circulation of the various current systems in the Asian-Australian region, with a strong focus on the circulation in the Indonesian Seas.

2.3 SEAPOM

SEAPOM is a configuration of the Princeton Ocean Model (POM) for the waters off southeast Australia. SEAPOM has a free surface and solves the non-linear primitive equations on a horizontal orthogonal curvilinear grid and a vertical sigma (terrain following) coordinate system using finite difference methods (Blumberg and Mellor, 1987). The variables u, v and w correspond to cross-shore (x direction), along-shore (y direction), and normal to the sigma surfaces velocity components respectively. The x/y grid orientation is approximately shore normal/shore parallel everywhere. The primitive variables are solved on an Arakawa-C staggered grid such that u is computed in the centre of the western boundary, v is computed in the centre of the southern boundary and w and variables related to turbulent kinetic energy are computed in the centre of the grid cell on the bottom face. Temperature, salinity, and surface elevation are solved in the centre point of the grid cell.

The version of the POM used (*circa* 2003) includes the Craig and Banner (1994) scheme for calculating the wave-driven flux of turbulent kinetic energy at the surface and a hydrostatic correction term for sigma-coordinate models (Chu and Fan, 2003). The Smagorinsky (1963) scheme is utilised in calculating horizontal diffusion and is applied with an inverse turbulent Prandtl number (TPRNI) of 1.0 and a horizontal diffusivity coefficient (HORCON) of 0.1. Temperature and salinity are advected using three iterations of the Smolarkiewicz upstream advection scheme (Smolarkiewicz, 1984). Coastal boundary conditions are: zero normal velocity, free slip tangential velocity and zero gradient for vertical velocity, temperature and salinity.

The physical configuration (Fig. 1) extends along the NSW coast from 28°24′S to 37°30′S, a distance of 1025 km, and extends offshore between 395 km (at 28°24′S) and 500 km (at 37°30′S). The grid for the model has 130 points in the cross-shore direction with a resolution between 1 and 6 km, and 325 points in

the along-shore direction with a resolution between 1.5 and 6 km. The outer six boxes on the northern, eastern and southern boundaries have smoothed topographies and a tapered wind stress to reduce unwanted boundary effects.

Along the eastern and southern boundaries a volume constraining radiation boundary condition with relaxation that permits oblique waves to radiate outwards (Marchesiello et al., 2001) is applied to elevation and the baroclinic horizontal velocity components. For the barotropic horizontal velocity components the Flather condition is applied (Flather, 1976). The model is forced with daily-averaged winds and radiative fluxes from the 2° NCAR 40-year reanalysis project (Kalnay et al., 1996).

The vertical sigma coordinates contains 36 levels, with greater resolution in the top and bottom boundary layers. Model depth and coastline are based on a global $2'$ bathymetry produced at the Naval Research Laboratory (NRL). The minimum and maximum depths are set at 15 m and 2000 m respectively. A minimum depth of 15 m reduces numerical instability along the coastline while a maximum depth of 2000 m (rather than the actual maximum depth of $>$ 4000 m) increases the allowable time step while not significantly influencing the model results (Oke and Middleton, 2001). The circulation model solves the external (barotropic) mode with a 1.7 s timestep and the internal (baroclinic) mode with a 60 s timestep.

2.3.1 Comparison of model grids

Fig. 2A compares the SEAPOM curvilinear ∼3 km resolution grid with the BRAN polar 0.1^o resolution grid for a region around Port Stephens where the EAC typically separates from the coast, and shelf processes are particularly important. In addition to higher resolution, the SEAPOM grid has a significant advantage over the BRAN grid as a result of being oriented cross-shore/along-shore which is aligned with the dominant currents for the length

of the NSW coast (Fig. 2A). Additionally, the coastline itself is better resolved as the curvilinear ocean-land interface is more generally along the coast when compared with the BRAN polar grid. Both model bathymetries are based on the NRL 2′ (∼3-3.6 km) data. The SEAPOM grid is slightly more resolved than the 2′ bathymetry data in the shallow regions, and, as a result, the SEAPOM grid coastline is occasionally one grid cell displaced from the more accurate coastline shown in Fig. 2A. This mismatch is small but could be eliminated with the use of a 1′ or less resolution bathymetry in the near shore regions.

The 36 layer vertical sigma coordinate system of SEAPOM gives improved vertical resolution in shallow, shelf regions (Fig. 2B). At the 200 m isobath, the maximum layer thickness is 8.7 m, compared to the BRAN grid of 10 m. Shallower than 230 m, the SEAPOM grid has thinner layer thickness than BRAN throughout the water column. The vertical sigma coordinate system, like the horizontal curvilinear grid, is favourably oriented for capturing along grid processes that occur on the shelf such as bottom boundary transport. Uplift of slope water through bottom boundary layer transport is known to be important on the NSW shelf (Oke and Middleton, 2001).

In the deepest (> 2000 m) regions, at depths between 50-740 m, the SEAPOM grid has vertical layers with a thickness of 43 m, while the BRAN grid has layers with a constant 10 m thickness in the top 200 m (Fig. 2B). As the total depth shallows, the maximum layer thickness in SEAPOM reduces, such that at 230 m of depth the maximum thickness is ∼10 m. Thus, the surface mixed layer is better resolved by SEAPOM in waters shallow than 230 m, and by BRAN for deeper waters.

2.4 Model initialisation

The model initialisation for SEAPOM consists of two stages. Stage 1 is diagnostic, where temperature and salinity are initially set to BODAS fields, and held constant while allowing velocity to evolve. Forcing functions such as solar radiation and winds are also held constant. Numerical experiments (not shown) reveal that kinetic and potential energy increase for up to 20 days before stabilising. As a result, a 20 day duration has been used in Stage 1 for all simulations. Stage 2 is prognostic, where temperature and salinity are allowed to evolve and are relaxed to the BODAS data following the assimilation cycle described below. Additional numerical experiments (not shown) reveal that up to two assimilation cycles are required before the RMS errors stabilise. Stage 2 therefore begins 14 days before the first reported results, and is forced with daily varying wind and radiative fluxes.

2.5 Data assimilation

BODAS temperature and salinity fields are available as a daily-mean every 7 days. The SEAPOM assimilation cycle involves relaxing to BODAS for a period (later shown ideally to be one day) centred on midday of the BODAS output day. For the rest of the 7-day cycle, model integration occurs without relaxation. The SEAPOM temperature and salinity fields are relaxed to BODAS fields based on the difference between the daily-mean BODAS field and the time-evolving POM field. The relaxation term is given by:

$$\frac{\partial T(t,s)}{\partial t}|_{relax} = \phi(s)\left(T_{SEAPOM}(t,s) - T_{BODAS}(s)\right)/\tau \qquad (1)$$

where t is time, s is space, $T_{SEAPOM}(t,s)$ is the instantaneous value of the POM configuration temperature field and is evaluated every 60 seconds, $T_{BODAS}(s)$ is the daily-mean temperature field of the analysis, τ is the time-scale for as-

similation, and $\phi(s)$ is a factor between 0 and 1 that optionally tapers the assimilation strength in shallow water. In simulations with tapered assimilation, the factor $\phi(s)$ varies horizontally and is a function of total water depth, H:

$$\phi(s) = \min[(H(s)/400)^2, 1]) \quad (2)$$

To horizontally smooth the assimilation strength, H is given by the mean depth of the grid box and its 8 surrounding neighbours. For untapered assimilation in shallow water $\phi(s) = 1$ everywhere. For both tapered and untapered simulations, boundary boxes (within 6 cells of the northern, eastern and southern boundary) have $\phi = 1$ independent of depth. In Sec. 3.1 the optimal time scale, τ, and duration of the assimilation are investigated.

2.6 In situ observations from September 2004

A research cruise from the 3 - 13 September 2004 on the Southern Surveyor (cruise number SS200408; Baird et al. (2008)) deployed a towed undulating device (SeaSoar) that measured temperature and salinity, while the shipboard ADCP measured depth-resolved velocity. The SeaSoar moved between the surface and 120 m (depth permitting). The ADCP velocities reported are relative to the bottom (i.e. corrected for ship movement).

2.7 SST data

The assessment of the downscaling of the 0.1° Bluelink ocean modelling outputs to a ∼3 km regional ocean model is made difficult by the errors in the SST products. Initially CSIRO 3-day AVHRR SST1m composites, that are available from the beginning of the BRAN simulations in 1992, were used. In a comparison of SST products with *in situ* temperature data, Beggs (2007)

found the mean and standard deviation ($\mu \pm \sigma$) of CSIRO 3-day composite AVHRR minus buoy observation for a broad region around Australia was - 0.01 $\pm$ 0.62°C. When compared to model predictions with errors of $\sim$1.0°C, the 3-day composite AVHRR errors of $\sim$0.62°C are significant. Despite the length of the AVHRR data set, it was concluded that it was best to use the LBoMSST and especially the RAMSSA data sets described below. Even with these more sophisticated products, up to one third of the RMS error estimates of SST in BODAS, BRAN and SEAPOM are due to errors in the observed SST.

For model assessment, the primary SST products used are:

(1) The Integrated Marine Observing System (IMOS) archived Legacy Bureau of Meteorology SST "Mosaic" (LBoMSST) is a 0.01° x 0.01° gridded composite product from 1.1 km High Resolution Picture Transmission (HRPT) Advanced Very High Resolution Radiometer (AVHRR) subskin ($\sim$1 mm) SST (SSTsubskin) from operational NOAA polar-orbiting satellites (Rea, 2004). This product is based on a running, weighted mean of observations over a 14 day period, with the most recent observations given the greatest weight.

(2) The Regional Australian Multi-Sensor SST Analysis (RAMSSA) is a 1/12° Optimal Interpolation SST analysis over the Australian region that combines infrared and microwave sensor observations with *in situ* measurements to produce daily SST estimates of "foundation" SST (SSTfnd) with the effects of nocturnal cooling and diurnal warming largely removed. The Gamma Test (and equivalent operational 1.0) versions of RAMSSA (Beggs, 2007), available from the 12 June 2006 to 26 October 2007, were used.

A comparison with *in situ* buoy observations over the region 60°E - 180°E, 20°N - 65°S from 1 October 2007 to 31 March 2008 gave bias and standard deviations of 0.0 $\pm$ 0.4°C for RAMSSA (pers comm. Helen Beggs). The SST products that do not remove the effects of nocturnal cooling and diurnal warm-

ing, such as LBoMSST, are noisier.

3 Results

3.1 Assimilation strategy assessment

In order to determine the best assimilation strategy for SEAPOM, a set of simulations with assimilation durations of 3, 12 and 24 hours and assimilation coefficients, τ, of 0.25, 0.5, 1 and 2 d^{-1} (Eq. 1) are undertaken . The simulations began on the 18 August 2004 and error statistics were calculated daily and spatially-averaged for both the continental shelf and the whole domain for the 6 weeks following the 1 September 2004, with tapering of assimilation effort on the shelf. The RMS errors of SEAPOM when compared to the LBoMSST product gave the best results on the continental shelf for $\tau = 1$ d^{-1} applied for 24 hours (Table 2). Off the shelf a reduced strength ($\tau = 0.5$ d^{-1}) slightly decreased errors. Given that the aim of the downscaling is improved performance on the shelf, and that BRAN also employed $\tau = 1$ d^{-1} applied for 24 hours, this strategy was used for all subsequent simulations.

3.2 Comparison with SST products

The comparison with SST products includes both calculation of the average RMS errors for seasons and model regions, and for averages through the 7-day assimilation cycle. For comparison of BRAN and SEAPOM, which have model outputs once daily, model day and observation day can be matched. The BODAS analysis is undertaken only every 7 days. For days that do not have an analysis, comparison is made with the last analysis undertaken. This is referred to as persistence (i.e. comparison of an estimate of SST for an earlier day with the present day observed value).

In addition to assessing the SEAPOM integration against SST products, SEAPOM persistence is also calculated. SEAPOM persistence does not take advantage of the SEAPOM integration over the days following the assimilation. However, the state at the end of the assimilation period is still strongly influenced by the model integration over the previous 7 days. An assimilation strength of 1 d^{-1} implies the model output is ∼37 % model determined and ∼63 % data constrained. The big advantage of persistence is that it is free of initialisation shock from the most recent assimilation period.

3.2.1 RAMSSA SSTfnd for winter 2006

In terms of spatial resolution and comparison with *in situ* observations, the best available SST product tuned for the Australian region is the RAMSSA SSTfnd analysis, which is available for June 2006 onwards. The RMS errors for winter 2006 for the continental shelf and whole domain with shelf-tapered and untapered assimilation are summarised in Table 3. The winter of 2006 was a time with a strong poleward extension of the EAC and therefore remote forcing of shelf waters. At this time SEAPOM performance is best with an untapered shelf assimilation strategy, and achieved a reduction of RMS error on the shelf of 0.13°C and 0.22°C relative to BRAN and BODAS respectively. As RAMMSA SST is only available for winter 2006, LBoMSST is used for 2002-2006, for which the comparison is restricted to the better performing untapered assimilation strategy.

3.2.2 LBoMSST for 2002-2006

The RMS errors of BODAS, BRAN and SEAPOM are assessed against LBoMSST for 9 weeks starting in the June and December of years 2002-2006 (actually December 2001-2005 for the summers of 2001/2 - 2005/6, but referred to as summers 2002-2006). The average over the 9 weeks of the RMS errors for

each day of the 7-day assimilation cycle are plotted for winter (Fig. 3) and summer (Fig. 4) for each year. On the shelf in winter the relaxation effort (reduction in RMS error during assimilation period due to relaxation) is small, and the RMS errors for SEAPOM remain fairly steady over the 7-day cycle (Fig. 3A-F). In contrast, for the whole domain SEAPOM RMS errors increase by $\sim$0.2°C through the 7 days, and require a larger relaxation effort.

In summer SEAPOM RMS errors also increase through the 7-day assimilation cycle, both on the shelf (Fig. 4A-F) and throughout the whole domain (Fig. 4G-L), although like winter the increase is less on the shelf. BRAN similarly required greater assimilation effort off the shelf and in summer. While on average SEAPOM performs better than BRAN, the assimilation effort as measured by the change in RMS errors between Day 1 and 2 are similar.

The average RMS errors based on nine 7-day assimilation cycles for winter and summer each year of SEAPOM, BRAN and BODAS on the shelf and for the whole domain are given in Table 4. RMS errors for all models are worse on the shelf than over the whole domain, and for summer compared to winter. This worse performance in summer versus winter partly reflects the 0.3°C greater variability in LBoMSST for summer compared to winter (Table 4). In contrast, for both summer and winter, the shelf and the whole domain have similar LBoMSST variability, but the models perform worse on the shelf.

SEAPOM performs better than BRAN on the shelf in winter for all years, improving the mean RMS errors by 0.11°C. The mean RMS errors for SEAPOM for whole domain in winter improve on BRAN by only 0.03°C, and are worse in three of the 5 years. In summer on the shelf SEAPOM is 0.04°C worse, and for the whole domain 0.03°C better.

The best estimate of SST on the shelf in 5 of the 10 seasons is achieved by SEAPOM, with 3 by SEAPOM persistence and 2 by BRAN. The persistence of analysis (BODAS) never records the lowest RMS errors on the shelf indicat-

ing that both the downscaling exercise, and model integration, are important for capturing shelf dynamics. In contrast, off the shelf SEAPOM persistence achieves the lowest RMS errors in 8 of the 10 seasons, with BODAS recording the other two. In the open ocean, where processes are less dynamic, the cost of model integration in terms of initialisation shock is greater than the gain of simulating 7 days. This was also found to be the case for BRAN versus BRAN persistence for southeast Australia (Fig. 12d of Oke et al. (2008)).

3.3 Comparison with in situ observations from September 2004

The 2004 Southern Surveyor cruise included transects across the Tasman Front at 152°E, 153°E and 153°30′E, and a shore normal shelf transect at Diamond Head, 31°45′ (Fig. 1). The surface temperature and velocity fields for BODAS, BRAN and SEAPOM for the region are shown in Fig. 5. Superimposed are the surface (∼20 m depth) ADCP velocities along the four transects. BRAN, BODAS and SEAPOM all place the EAC at approximately the same distance offshore at Diamond Head, in agreement with observations (see below). In contrast, there is some disagreement between the *in situ* observations of the location of the offshore fronts and those of BODAS, BRAN and SEAPOM. The ADCP transects were centred on the observed thermal fronts. While the location of the thermal front at 153°E in BRAN is in agreement with observations, the orientation of the current is not (Fig. 5B). As a result, the downstream front at 153°30′E in BRAN appears 46 km too far south. Neither SEAPOM nor BRAN form the thermal front that was observed at 152°E. In order to compare the structure of thermal fronts formed along 153°30′E, the below analysis compares the *in situ* observations and SEAPOM at the same latitude as the observations, and BRAN from 46 km further south.

3.3.1 Shelf processes

The ability of SEAPOM to resolve continental shelf properties is illustrated by a transect off Diamond Head (Fig. 6). The observations (Fig. 6C) show cool slope water has been lifted onto the continental shelf, with 16°C water seen as shallow as 60 m at 12 km offshore. In the BRAN integration (Fig. 6B) this water has fallen to 135 m since the last relaxation period. In contrast, the SEAPOM integration has 16°C water at 70 m and isotherms are lifted right up to the coast (Fig. 6D), suggesting the sigma co-ordinate grid is better suited to the shelf density profile. The offshore location of the 19.5°C isotherm at the surface representing the thermal front is well positioned in each simulation, however the temperature maximum in the core of the EAC is too high, especially in SEAPOM (Fig. 6D). Neither simulation captures the wave-like structure of the thermocline seen in the observations (Fig. 6C).

The observed northward component of the velocity field of the 6 September 2004 (Fig. 6C) shows a maximum southward current of 0.4 m s^{-1} at 20-50 m depth and 20 km offshore (the shipboard ADCP does not have measurements for the top 20 m). In the bottom waters of the continental shelf the velocities decrease to less than 0.2 m s^{-1} southward. Off the continental shelf the southward currents reduce from the 0.4 m s^{-1} maximum to $\sim$0.2 m s^{-1}. SEAPOM does an excellent job of capturing the onshelf velocity field. The current is less than 0.2 m s^{-1} southward close to the bottom and coast, and has a similar maximum at approximately the same distance offshore. A region of 0.6 m s^{-1} southward currents are evident in SEAPOM above 20 m (Fig. 6D), but cannot be assessed against the observations that are not resolved in the top 20 m. However, off the shelf SEAPOM overestimates the southward velocities. The BRAN velocity field generally captures the shape of the observations. While BRAN overestimates shelf velocities, particularly at depth and close to the coast, the offshelf velocity field is more realistic than SEAPOM.

3.3.2 Tasman Front

The boundary between warm Coral Sea waters and cool Tasman Sea waters, the Tasman Front, forms an eastward flowing jet between 31°S and 37°S. The formation of the Tasman Front in the model simulations is assessed using a transect at 153°30′E on the 3 September 2004 (Fig. 7). Between temperatures of 17.5°C and 19°C, the observed surface temperature gradient is $\sim$0.4°C km^{-1} (Fig. 7C and Baird et al. (2008)). For the same temperature range (slightly displaced in the model outputs), BODAS and BRAN both have a gradient of 0.03°C km^{-1} while SEAPOM has a gradient of 0.09°C km^{-1}. The factor of 3 greater spatial resolution of SEAPOM allows an approximately factor of 3 sharpening of the thermal front, and better resolution of the frontal jet (Fig. 7). Although the temperature gradient is not as sharp as observed, SEAPOM has approximately the correct magnitude of along front velocities, and slope of the isotherms. BRAN, in contrast, has such weak temperature gradients that no concentration of along front current emerges.

4 Discussion

When moving from the coarse resolution BRAN model to the finer resolution SEAPOM, it might be expected that smaller scale features would be better resolved in a qualitative sense, but that circulation (as measured by RMS errors in SST) be degraded in a quantitative sense. That is, the higher resolution model may have add noise to the large scale signal that is being quantified in SST RMS errors. Instead we find that SEAPOM resolves finer scale features with no quantitative degradation in broad scale performance.

SEAPOM performed better on the shelf in winter than summer, and worst of all in the summer of 2006. To illustrate this performance, LBoMSST, BRAN, BODAS and SEAPOM are compared on the 7 June 2003 (Fig. 8) and

the 2nd January 2006 (Fig. 9). On the 7 June 2003, BRAN and SEAPOM were similar, with relatively low RMS errors for the continental shelf, and SST fields that well capture the observations. The main source of error in BRAN and SEAPOM is the cooler coastal waters between 29°S-31°S relative to LBoMSST.

Cooler water between 29°S-31°S relative to LBoMSST is also present in the model SST fields for the 2 January 2006 (Fig. 9), and is the reason for their poor performance. The LBoMSST field suggests that no upwelled water is reaching the surface (Fig. 9), despite the strong upwelling favourable winds evident in both the NCEP 2° winds that forced SEAPOM (not shown), and the observed 10 m winds from the QuikSCAT satellite (Fig. 10). Persistent winds of up to 15 m s^{-1} in a northerly, alongshore direction in the region are sufficiently strong to bring upwelled water to the surface, as seen in November 1998 (Roughan and Middleton, 2002).

While LBoMSST, an AVHRR-based SST product based on a weighted 14 day window shows very little upwelling on the 2 January 2006, the CSIRO 3-day AVHRR composite (Fig. 10) does show 20°C water at the surface at 32°S. It may be that the intermittent nature of upwelling events is not well captured by the LBoMSST product, even though on average its errors are smaller than the CSIRO 3-day AVHRR composite. If the CSIRO 3-day AVHRR composite is more realistic on 2 January 2006, then BRAN would appear to have the upwelling intensity approximately correct, with SEAPOM over estimating the effect upwelling on SST by perhaps a 1°C.

A spatially-resolved image of SST bias of SEAPOM and BRAN relative to LBoMSST in both summer and winter reveals that both models are too cool on the northern continental shelf (Fig. 11), with BRAN in summer being the worst (Fig. 11C). The general trends of SST bias are quite similar for both BRAN and SEAPOM (compare Fig. 11A & B with Fig. 11C & D) and for BODAS

(not shown), illustrating that the relaxation to BODAS is quite strong. The standard deviation of LBoMSST - model SST are less for SEAPOM than BRAN which is another metric of the improvement the downscaled SEAPOM achieves.

A considerable component of the poorer results in summer can be attributed to local versus remote forcing. The East Australian Current has a maximum transport at 30°S in summer (Ridgway and Godfrey, 1997). The poleward extension of the EAC, forcing water along the NSW shelf south of the separation point, also has a maximum in summer. In contrast, local winds have a maximum in winter. Of the summer years, 2006 had a particularly strong poleward extension, and has by far the worst errors. Off the shelf, however, BODAS and BRAN did not do any worse in 2006 (Table 4). Remote forcing, interacting with the shelf, appears to be most difficult processes to incorporate into circulation models of the NSW shelf.

SEAPOM Persistence is a best estimate of SST for the whole domain for 8 of the 10 integrations (Table 4). This appears to be due to an initialisation shock that occurs after assimilation. The RMS errors of the SEAPOM integration for the whole domain quickly degrades after assimilation, before stabilising (Fig. 4). The strategy of assimilating data for 1 day every 7 days was chosen to match the BRAN 7-day assimilation strategy, and the outcome of experiments in Sec. 3.1. For the use of SEAPOM predictions off the shelf, the best performance may be obtained by assimilating data less often (say every 2-3 weeks).

In this paper the primary means of regional scale assessment of the downscale model performance has been the use of high-resolution SST products. Applications of the downscaled model for use in particle distribution and biological responses depend primarily on the current field. The assessment of current fields using ship-board ADCP transects showed improved representation of

frontal features in SEAPOM, although assessment is limited to one period of time. While data does not exist to make a comparison of surface velocity fields, it is still worth commenting on the local current fields that develop in SEAPOM.

To illustrate differences, the surface velocity field for BRAN and SEAPOM on the 10 August 2004 are used (Fig. 12). For the region shown in Fig. 12, the RMS errors compared to LBoMSST of BRAN were 1.26°C and 1.22°C for SEAPOM. The broad-scale patterns of a strong warm southward flowing current off the shelf, and a cooler northward flowing counter-current on the shelf can be seen in both SEAPOM and BRAN. The relatively large RMS errors for the region occur because the EAC waters for both BRAN and SEAPOM are too warm. On the shelf, SEAPOM forms 4 small eddies, while BRAN produces only one relatively large rotating cell. In particular, the 0.1° BRAN configuration does not produce the strong cyclonic circulation south of Port Stephens in the Stockton Bight (33°S) that is regularly observed and believed to be important in creating a nursery for pelagic fish stocks (I. Suthers, pers. comm.). In any case, RMS errors of SST, the main data set available for model assessment, is not a good metric for judging the abilities to resolve shelf currents, perhaps the most important feature required of a downscaled model. The planned installation of a coastal radar on the northern NSW coast may in the future provide the data needed for a more thorough assessment of model shelf circulation.

4.1 Summary

The downscaling of Bluelink products to a ∼3 km resolution shelf model is shown to have modest quantitative improvements in estimations of SST, being most effective on the shelf and in winter. *In situ* observations provide a higher spatial resolution for assessment, and suggest that shelf and frontal features

are better captured by the downscaled model. Apart from these modest but significant improvements, SEAPOM produced believable but difficult to assess fine scale shelf currents without degrading the larger scale features that are assessable. Previous applications (Marchesiello and Middleton, 2000; Oke and Middleton, 2001; Roughan et al., 2003; Baird et al., 2006a, 2007; Macdonald et al., 2009) of the southeast Australian configuration of the POM have been used to reproduce events in a qualitative sense. The present demonstration of quantitative reproduction of circulation over longer durations introduces the potential for quantitative inter-annual modelling applications such as coastal connectivity, and biological and chemical modelling.

5 Acknowledgements

We thank Alan Blumberg and George Mellor for the free availability of the Princeton Ocean Model (POM), Jason Middleton and his group (esp. Patrick Timko) at UNSW for the development of the NSW POM configuration, and the CSIRO, BOM and RAN Bluelink Project for the free availability of the BODAS and BRAN products. We thank Helen Beggs of BOM for help with using the SST products. Bluelink and BoM provided the RAMSSA SST analyses. BoM and the Integrated Marine Observing System (IMOS) - an initiative of the Australian Government being conducted as part of the National Collaborative Research Infrastructure Strategy - provided the LBoMSST product. MB is funded through ARC Discovery Grant DP0557618. MR and HM were partially funded through the New South Wales Department of Primary Industries to assist with a marine pest risk assessment, using funding from the Sydney Metropolitan Catchment Management Authority. We are particularly grateful to Duncan Smith, Martin Thompson and Michael Jansen for their engineering of the UNSW condor cluster, and the staff and students of the School of Mathematics and Statistics on whose idle desktop computers the simula-

tions ran. Finally, thank you to the crew of the 2004 Southern Surveyor cruise, and in particular to Jason Middleton, Iain Suthers, Patrick Timko, Deborah Cox, Tom Mullaney, Lindsay Pender, Drew Mills and Mark Underwood for the collection of *in situ* data used for model assessment.

References

Ajani, P., Hallegraeff, G. M., Pritchard, T., 2001. Historic overview of algal blooms in marine and estuarine waters of New South Wales, Australia. Proc. Linn. Soc. N.S.W. 123, 1–22.

Baird, M. E., Timko, P. G., Suthers, I. M., Middleton, J. H., 2006a. Coupled physical-biological modelling study of the East Australian Current with idealised wind forcing. Part I: Biological model intercomparison. J. Mar. Sys. 59, 249–270.

Baird, M. E., Timko, P. G., Suthers, I. M., Middleton, J. H., 2006b. Coupled physical-biological modelling study of the East Australian Current with idealised wind forcing: Part II: Biological dynamical analysis. J. Mar. Sys. 59, 271–291.

Baird, M. E., Timko, P. G., Suthers, I. M., Middleton, J. H., Mullaney, T. J., Cox, D. R., 2008. Analysis of biological properties across the Tasman Front off south east Australia. Deep-Sea Res. 55, 1438–1455.

Baird, M. E., Timko, P. G., Wu, L., 2007. The effect of packaging of chlorophyll within phytoplankton and light scattering in a coupled physical-biological ocean model. Mar. Fresh. Res. 58, 966–981.

Banks, S. C., Piggott, M. P., Williamson, J. E., Bove, U., Holbrook, N. J., Beheregaray, L. B., 2007. Oceanic variability and coastal topography share genetic structure in a long-dispersing sea urchin. Ecology 88, 3055–3064.

Beggs, H., 2007. A high-resolution blended sea surface temperature analysis over the Australian region. Tech. rep., Bureau of Meteorology Research Centre, BMRC Research Report No. 130.

584 Blumberg, A. F., Mellor, G. L., 1987. A description of a three-dimensional
585 coastal ocean circulation model. In: Heaps, N. (Ed.), Three-dimensional
586 Coastal Ocean Models. American Geophysical Union, pp. 1–15.
587 Booth, D. J., Figueira, W. F., Gregson, M. A., Brown, L., Beretta, G., 2007.
588 Occurrence of tropical fishes in temperate southeastern Australia: Role of
589 the East Australian Current. Est. Coast. Shelf Sci. 72, 102–114.
590 Chu, P. C., Fan, C., 2003. Hydrostatic correction for sigma coordinate ocean
591 models. J. Geophys. Res. 108(C6), 3206.
592 Craig, P. D., Banner, M. L., 1994. Modeling wave-enhanced turbulence in the
593 ocean surface layer. J. Phys. Oceanogr. 24, 2546–2559.
594 Cresswell, G. R., Legeckis, R., 1986. Eddies off southeastern Australia. Deep-
595 Sea Res. 33, 1527–1562.
596 Flather, R., 1976. A tidal model of the northwest European continental shelf.
597 Mem. Soc. R. Sci. Liege 10, 141–164.
598 Griffies, S. M., Harrison, M. J., Pacanowski, R. C., Rosati, A., March 2004.
599 A technical guide to MOM4 GFDL Ocean Group Technical Report No. 5
600 Version prepared on March 3, 2004. Tech. rep., NOAA/Geophysical Fluid
601 Dynamics Laboratory.
602 Kalnay, E., Kanamitsu, M., Kistler, R., Collins, W., Deaven, D., Gandin,
603 L., Iredell, M., Saha, S., White, G., Woollen, J., Zhu, Y., Chelliah, M.,
604 Ebisuzaki, W., Higgins, W., Janowiak, J., Mo, K., Ropelewski, C., Wang,
605 J., Leetmaa, A., R., R., R., J., Joseph, D., 1996. The ncep/ncar 40-year
606 reanalysis project. Bulletin of the American Meteorological Society 77, 437–
607 471.
608 Macdonald, H. S., Baird, M. E., Middleton, J. H., 2009. The effect of wind on
609 continental shelf carbon fluxes off southeast Australia: a numerical model.
610 J. Geophys. Res. 114, C05016,doi:10.1029/2008JC004946.
611 Marchesiello, P., McWilliams, J. C., Shchepetkin, A., 2001. Open boundary
612 conditions for long-term integration of regional oceanic models. Ocean Mod-
613 elling 3, 1–20.

Marchesiello, P., Middleton, J. H., 2000. Modeling the East Australian Current in the Western Tasman Sea. J. Phys. Oceanogr. 30, 2956–2971.

NSW Marine Parks Authority, 2008. A review of benefits of marine protected areas and related zoning considerations. Tech. rep., NSW Marine Parks Authority.

Oke, P. R., Brassington, G. B., Griffin, D. A., Schiller, A., 2008. The Bluelink ocean data assimilation system (BODAS). Ocean Model. 21, 46–70.

Oke, P. R., Middleton, J. H., 2001. Nutrient enrichment off Port Stephens: the role of the East Australian Current. Cont. Shelf Res. 21, 587–606.

Oke, P. R., Schiller, A., Griffin, D. A., Brassington, G. B., 2005. Ensemble data assimilation for an eddy-resolving ocean model of the Australian Region. Q. J. Roy. Met. Soc. 131, 3301–331.

Pritchard, T., Ajani, P., Andrew, D., Calfas, M., Holden, C., Lee, R., Linforth, S., Rendell, P., 1997. Relative significance of slope water, estuarine discharges and sewage outfalls for nutrients in offshore coastal waters. In: Coastal Nutrients Workshop. Australian Water and Wastewater Association, Sydney, pp. 44–50.

Rea, A., 2004. Recent Improvements to the NOAA AVHRR SST Product at the Australian Bureau of Meteorology. Tech. rep., Australian Bureau of Meteorology, Presented to the Fifth GODAE High Resolution SST Pilot Project Science Team Workshop, Townsville, Australia, 25-30th July, 2004, http://www.bom.gov.au/bmrc/ocean/BLUElink/SST/5th_GHRSST-PP_Workshop_Paper-Anthony_Rea.doc.

Ridgway, K. R., Dunn, J. R., 2003. Mesoscale structure of the mean East Australian Current System and its relationship with topography. Prog. Oceanogr, 56, 189–222.

Ridgway, K. R., Godfrey, J. S., 1997. Seasonal cycle of the East Australian Current. J. Geophys. Res. 102, 921–936.

Roughan, M., Macdonald, H. S., Baird, M. E., in prep. Modelling connectivity in a western boundary current with applications to the East Australian

Current. .

Roughan, M., Middleton, J. H., 2002. A comparison of observed upwelling mechanisms off the east coast of Australia. Cont. Shelf Res. 22, 2551–2572.

Roughan, M., Oke, P. R., Middleton, J. H., 2003. A modeling study of the climatological current field and the trajectories of upwelled particles in the East Australia Current. J. Phys. Oceanogr. 33, 2551–2564.

Schiller, A., Oke, P. R., Brassington, G., Entel, M., Fiedler, R., Griffin, D. A., Mainsbrigde, J. V., 2008. Eddy-resolving ocean circulation in the Asian-Australian region inferred from an ocean reanalysis effort. Prog. Oceanogr. 76, 334–365.

Schiller, A., Ridgway, K. R., Steinberg, C. R., Oke, P. R., 2009. Dynamics of three anomalous SST events in the Coral Sea. Geophys. Res. Lett. 36, L06606, doi:10.1029/2008GL036997.

Smagorinsky, J., 1963. General circulation experiments with primitive equations. Mon. Wea. Rev. 91, 99–164.

Smolarkiewicz, P. K., 1984. A fully multidimensional positive definite advection transport algorithm with small implicit diffusion. J. Comput. Phys. 54, 325–362.

Sydney Water, November 2005. Sydney's desalination project. Tech. rep., Sydney Water.

Tilburg, C. E., Hurlburt, H. E., O'Brien, J. J., Shriver, J. Y., 2001. The dynamics of the East Australian Current System: The Tasman Front, the East Auckland Current, and the East Cape Current. J. Phys. Oceanogr. 31, 2917–2943.

ADCP	Acoustic Doppler Current Profiler
AMSR-E	Advanced Microwave Scanning Radiometer - Earth observing system
AVHRR	Advanced Very High Resolution Radiometer
Bluelink	Collaboration between CSIRO, BoM and RAN
BODAS	Bluelink Ocean Data Assimilation System
BoM	Bureau of Meteorology (Australia)
BRAN	Bluelink ReANalysis
CSIRO	Commonwealth Scientific and Industrial Research Organisation (Australia)
EAC	East Australian Current
IMOS	Integrated Marine Observing System (Australia)
LBoMSST	Legacy BoM SST
MOM	Modular Ocean Model
NCEP	National Centers for Environmental Prediction (USA)
NSW	New South Wales (state of Australia)
POM	Princeton Ocean Model
QuikSCAT	Sea winds estimated from NASA Scatterometer
RAMSSA	Regional Australian Multi-Sensor SST Analysis
RAN	Royal Australian Navy
RMS	Root Mean Square
SEAPOM	SouthEast Australian configuration of POM
SST	Sea Surface Temperature
SSTfnd	SST with diurnal effects removed

Table 1
Acronyms used in this paper.

	Duration (h)					
	Cont. Shelf			Whole D.		
Strength (d^{-1})	3	12	24	3	12.	24
0.25	1.01	0.989	1.02	0.972	0.902	0.936
0.5	1.04	0.985	0.982	1.09	0.894	0.882
1	1.04	0.969	**0.946**	1.15	0.926	**0.895**
2	1.12	0.966	0.987	1.25	0.968	0.888

Table 2
RMS error for model SST against LBoMSST for durations of 3, 12 and 24 hours and assimilation coefficient of 0.25, 0.5, 1 and 2 d^{-1}. The simulations began on the 18 August 2004 and error statistics were calculated daily and spatially averaged for both the continental shelf and the whole domain for the 6 weeks following the 1 September 2004, with tapering of assimilation effort on the shelf. RMS error is calculated daily and averaged for the 6 week period. The RMS errors for the strategy used in the rest of the study are in bold.

Coastal	Continental shelf				Whole domain			
assimilation	SEAPOM	SEAPOM P.	BRAN	BODAS	SEAPOM	SEAPOM P.	BRAN	BODAS
Untapered	0.853	0.88	0.981	1.07	0.868	0.708	0.981	0.86
Tapered	0.945	0.917	0.981	1.07	1.02	0.912	0.981	0.86

Table 3
The RMS error of SEAPOM, SEAPOM persistence, BRAN and BODAS when compared to RAMSSA SSTfnd for winter 2006.

	Continental Shelf					Whole Domain				
Year	SEAPOM	SEAPOM P.	BRAN	BODAS	Obs	SEAPOM	SEAPOM P.	BRAN	BODAS	Obs
W 2002	1.02†	**0.985**†	1.10	1.22	1.06	1.03†	**0.845**†	0.984†	0.890†	1.16
W 2003	**0.892**†	0.906†	1.02†	1.14†	1.21	0.855†	**0.747**†	0.963†	0.833†	1.14
W 2004	**1.03**†	1.04†	1.18	1.15†	1.17	0.913†	0.811†	0.886†	**0.775**†	1.05
W 2005	**1.14**	1.22	1.21	1.42	1.05	0.930†	**0.807**†	0.917†	0.872†	1.02
W 2006	**0.982**	0.998	1.13	1.17	0.742	1.04†	**0.878**†	1.13	0.946†	1.06
W mean	**1.01**†	1.03†	1.13	1.22	1.05	0.954†	**0.818**†	0.981†	0.863†	1.09
S 2002	1.30†	**1.10**†	1.17†	1.19†	1.47	1.12†	**0.993**†	1.21†	1.07†	1.42
S 2003	1.27†	**1.23**†	1.29†	1.39	1.34	1.07†	**0.914**†	1.09†	0.979†	1.18
S 2004	1.50	1.49	**1.47**	1.64	1.34	1.14†	1.06†	1.16†	**1.05**†	1.60
S 2005	**1.47**	1.54	1.49	1.65	1.30	1.14†	**1.02**†	1.17†	1.07†	1.34
S 2006	1.81	1.79	**1.72**	1.91	1.37	1.15†	**0.994**†	1.14†	1.07†	1.30
S mean	1.47	**1.43**	1.43	1.56	1.36	1.12†	**1.00**†	1.15†	1.05†	1.37

Table 4
The RMS error of SEAPOM, SEAPOM persistence, BRAN and BODAS when compared to LBoMSST for 2002, 2003, 2004, 2005 and 2006 in winter (W) and summer (S). The smallest RMS error for each season and region is in bold. The columns headed 'Obs' are the RMS difference between daily LBoMSST and the mean LBoMSST for the season and region given. Simulations that have less error than observed seasonal variability are noted with a †. The SEAPOM simulations had untapered relaxation on the continental shelf.

Fig. 1. The regional bathymetry and SEAPOM horizontal grid. The insert shows the location of the study off the coast of southeast Australia. The white lines show every 10th grid line. A high resolution coastline is shown in black, with light shading signifying land cells in the model. The colour scale shows a $2'$ bathymetry used to calculate model depth. The 200 m isobath is shown in white. The boxed area shows the region plotted in Fig. 2 and Fig. 12. The location of the Tasman Front transect in Fig. 7 is shown in white and the Diamond Head transect in Fig. 6 in black.

Fig. 2. A. The Australian coastline (thick black line), the interface between land and ocean for the SEAPOM grid (thick dark grey) and for the BRAN grid (thick light grey). The polar BRAN grid (thin grey) and curvilinear SEAPOM grid (thin black) for the shelf near Port Stephens. B. Cross-shelf slice (shown as a dash-dot line in Panel A) with the SEAPOM sigma-coordinate grid (thin black lines) and model bathymetry (thick dark grey). A BRAN z-level grid of 0.1° horizontal resolution that would best resolve the SEAPOM slice is shown (thin light grey).

Fig. 3. The RMS error [°C] in winter for SEAPOM, SEAPOM persistence, BRAN and BODAS against LBoMSST on the continental shelf (top row) and for the whole domain (bottom row). Columns 1-5 show averages of RMS error for each day based on 9 consecutive 7-day assimilation cycles for 2002, 2003, 2004, 2005 and 2006. The 6th column shows the average of all years. Assimilation occurred between Days 1 and 2, as shown by the grey area.

Fig. 4. The RMS error [°C] in summer for SEAPOM, SEAPOM persistence, BRAN and BODAS against LBoMSST on the continental shelf (top row) and for the whole domain (bottom row). For more details see Fig. 3.

Fig. 5. Surface temperature (colour) and velocity (arrows) from: (A) BODAS analysis field at midday on the 1 September; (B) BRAN integration daily mean of the 5 September 2004; (C) SEAPOM at midday on the 5th September. ADCP measured surface ($\sim$20 m deep) velocities of the four transects of the Southern Surveyor cruise of 2004 at Diamond Head and across the observed Tasman Front (Baird et al., 2008) are shown in pink. Model velocity shown as the path of a particle in the velocity field for one day from the 5th September. The ADCP arrows are one day travel in a straight line. The grey line at 153°30′E in the centre panel shows the location of the BRAN section used to characterise the front in Fig. 7.

Fig. 6. Temperature (colour) and northward velocity (contours) fields along an E-W transect at 31°45′S in early September 2004. (A) BODAS analysis field at midday on the 1st of September; (B) BRAN integration daily mean of the 6th September 2004; (C) Observations from the Southern Surveyor undertaken in an easterly direction from 19:53 to 22:01 on the 6th September Eastern Standard Time using a towed undulating SeaSoar (path shown with dots, bottom topography from shipboard depth sounder) and shipboard ADCP; and (D) SEAPOM integration snapshot at 1200 on the 6th September. The observation region is shown on the model outputs as a thin black line, and the bottom topography as a thick white line. The x-axis is offshore distance.

Fig. 7. Temperature (colour) and eastward velocity (contours) fields along a N-S transect at 153°30′S in early September 2004. Distance is given from the beginning of the SeaSoar transect. The BRAN transect is shifted 46 km south in order to capture the same frontal features (Fig. 5). For more details see Fig. 6.

Fig. 8. SST for LBoMSST, BODAS, BRAN, and SEAPOM on the 7 June 2003 when the RMS errors of BRAN and SEAPOM were significantly less than BODAS. The 200 m isobath is shown as a black line. The RMS error for the continental shelf on this day is given for each model at the bottom of the panel.

Fig. 9. SST for LBoMSST, BODAS, BRAN, and SEAPOM on the 2 January 2006 when the RMS errors were large. For more details see Fig. 8.

Fig. 10. Observed QuikSCAT 10 m wind field and a 3-day composite CSIRO AVHRR SST for the 7 June 2003, the same time period as shown in Fig. 8.

Fig. 11. Spatially-resolved mean temperature difference [°C] between LBoMSST and SEAPOM (A & B) and BRAN (C & D) in summer (A & C) and winter (B & D) for 2002-2006. The mean (μ) and standard deviation (σ) for the whole domain for each model and season is given in the panels.

Fig. 12. Surface temperature and velocity fields for (A) SEAPOM and (B) BRAN for 10 August 2004 (6 days after assimilating BODAS). To emphasize resolution differences, the images contain the original model's resolution of both temperature and velocity. Velocity is given at the centre of the model grid cell, calculated from interpolation from the grid edges at which it is solved. For more information see Fig. 1.

Figure 1

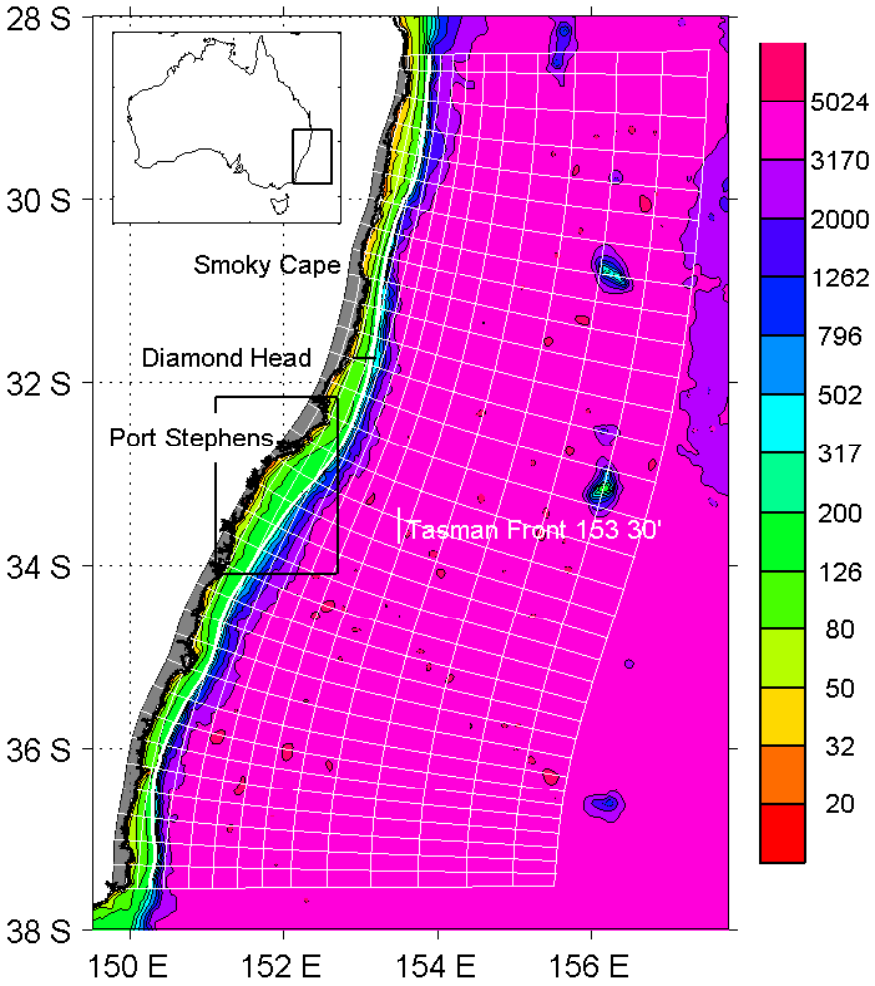
28 S
30 S
32 S
34 S
36 S
38 S
150 E
152 E
154 E
156 E
Smoky Cape
Diamond Head
Port Stephens
Tasman Front 153 30'
5024
3170
2000
1262
796
502
317
200
126
80
50
32
20

Figure 2

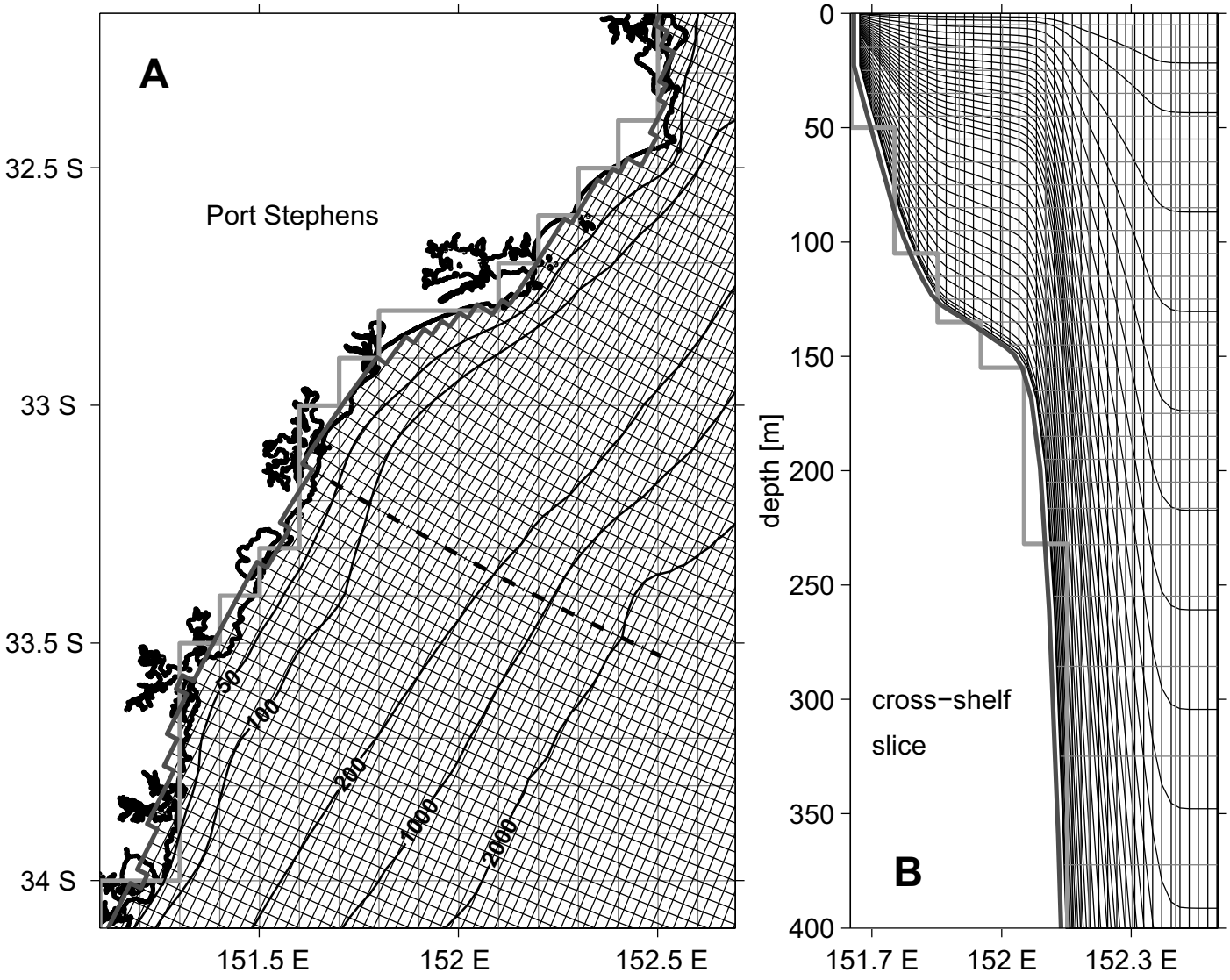
A
Port Stephens
32.5 S
33 S
33.5 S
34 S
151.5 E
152 E
152.5 E
50
100
200
1000
2000
B
cross−shelf
slice
depth [m]
0
50
100
150
200
250
300
350
400
151.7 E
152 E
152.3 E

Figure 3

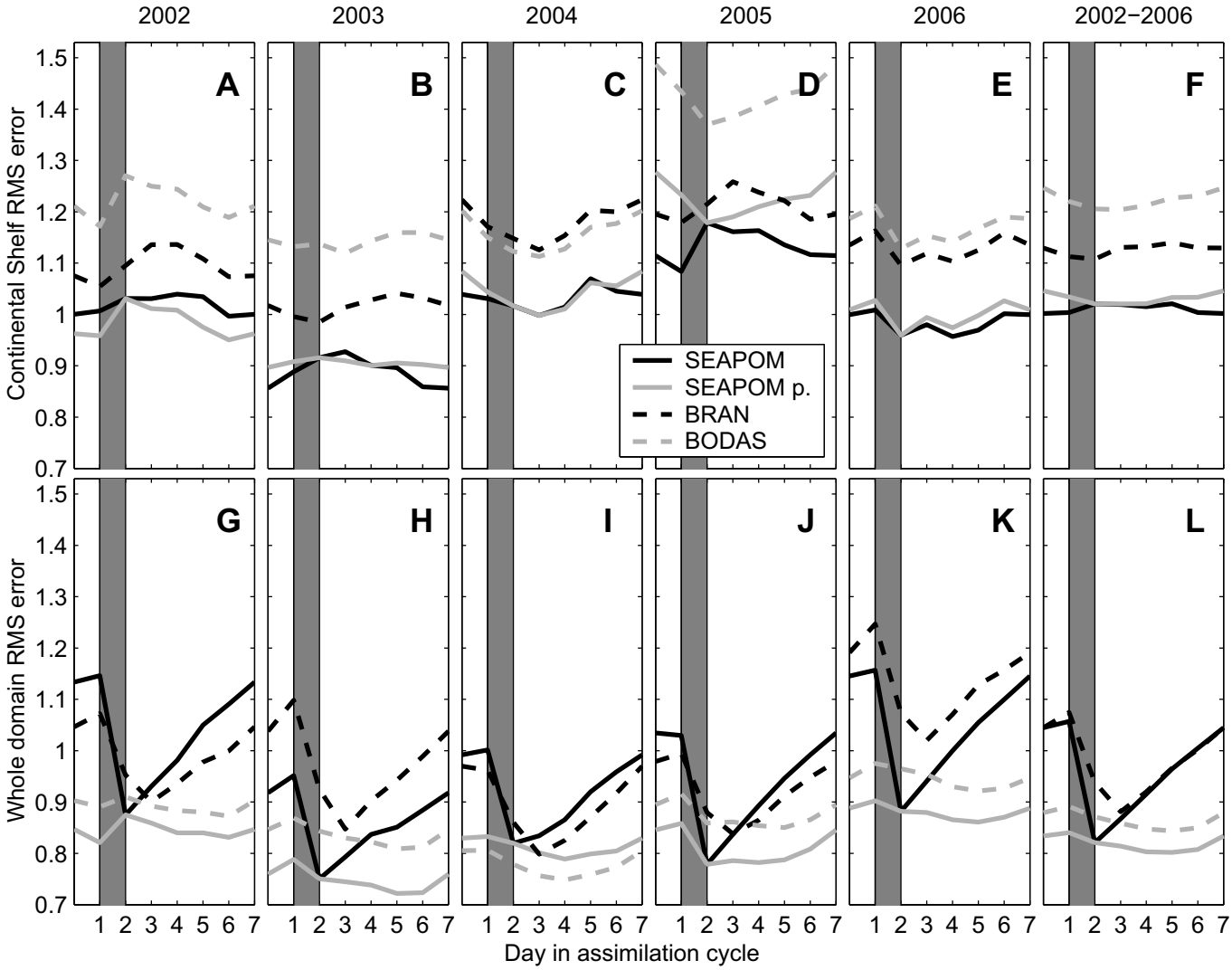
2002
2003
2004
2005
2006
2002−2006
A
B
C
D
E
F
G
H
I
J
K
L
Continental Shelf RMS error
Whole domain RMS error
Day in assimilation cycle
SEAPOM
SEAPOM p.
BRAN
BODAS
0.7
0.8
0.9
1
1.1
1.2
1.3
1.4
1.5
1 2 3 4 5 6 7

Figure 4

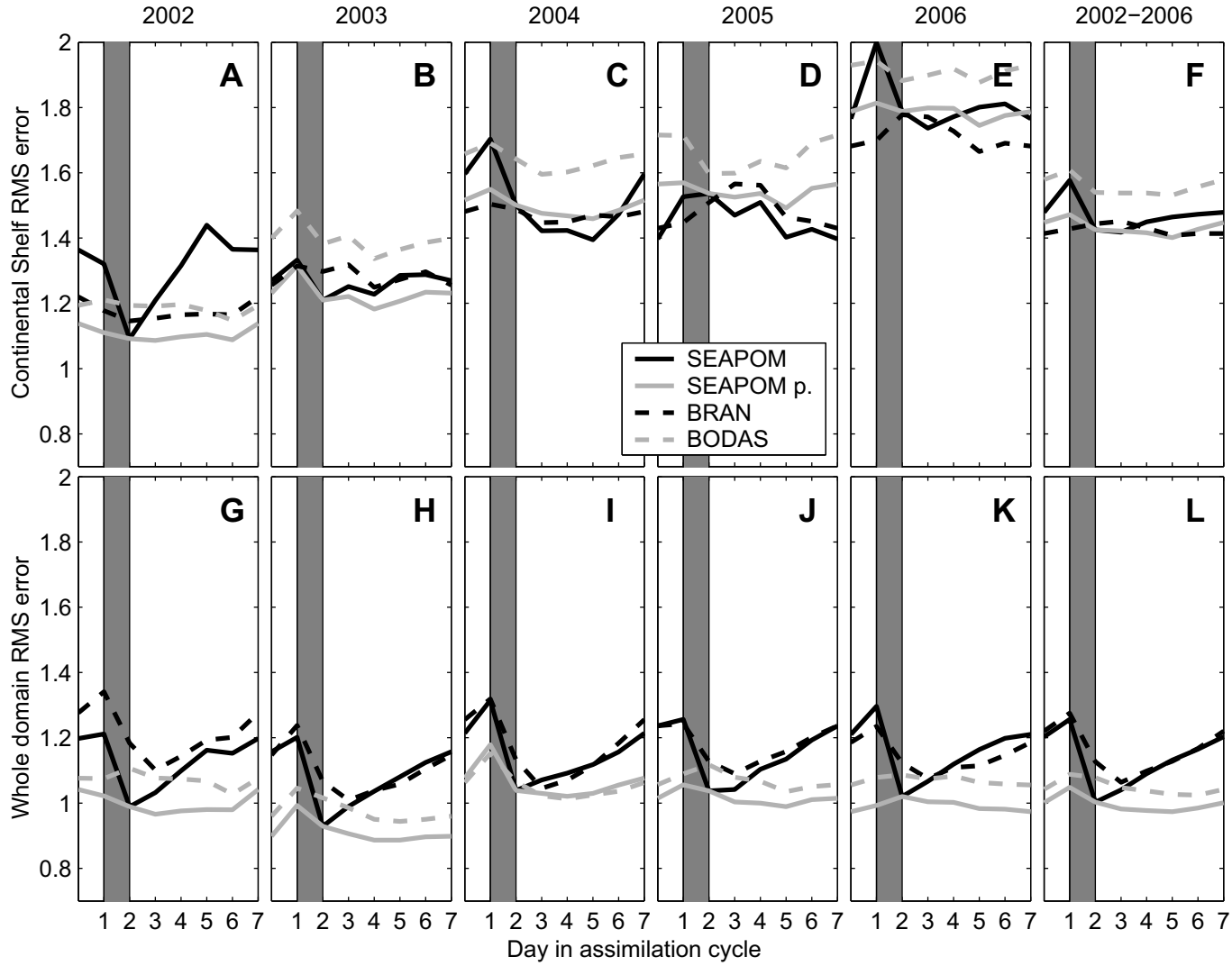
2002
2003
2004
2005
2006
2002−2006
A
B
C
D
E
F
G
H
I
J
K
L
Continental Shelf RMS error
Whole domain RMS error
SEAPOM
SEAPOM p.
BRAN
BODAS
Day in assimilation cycle

Figure 5

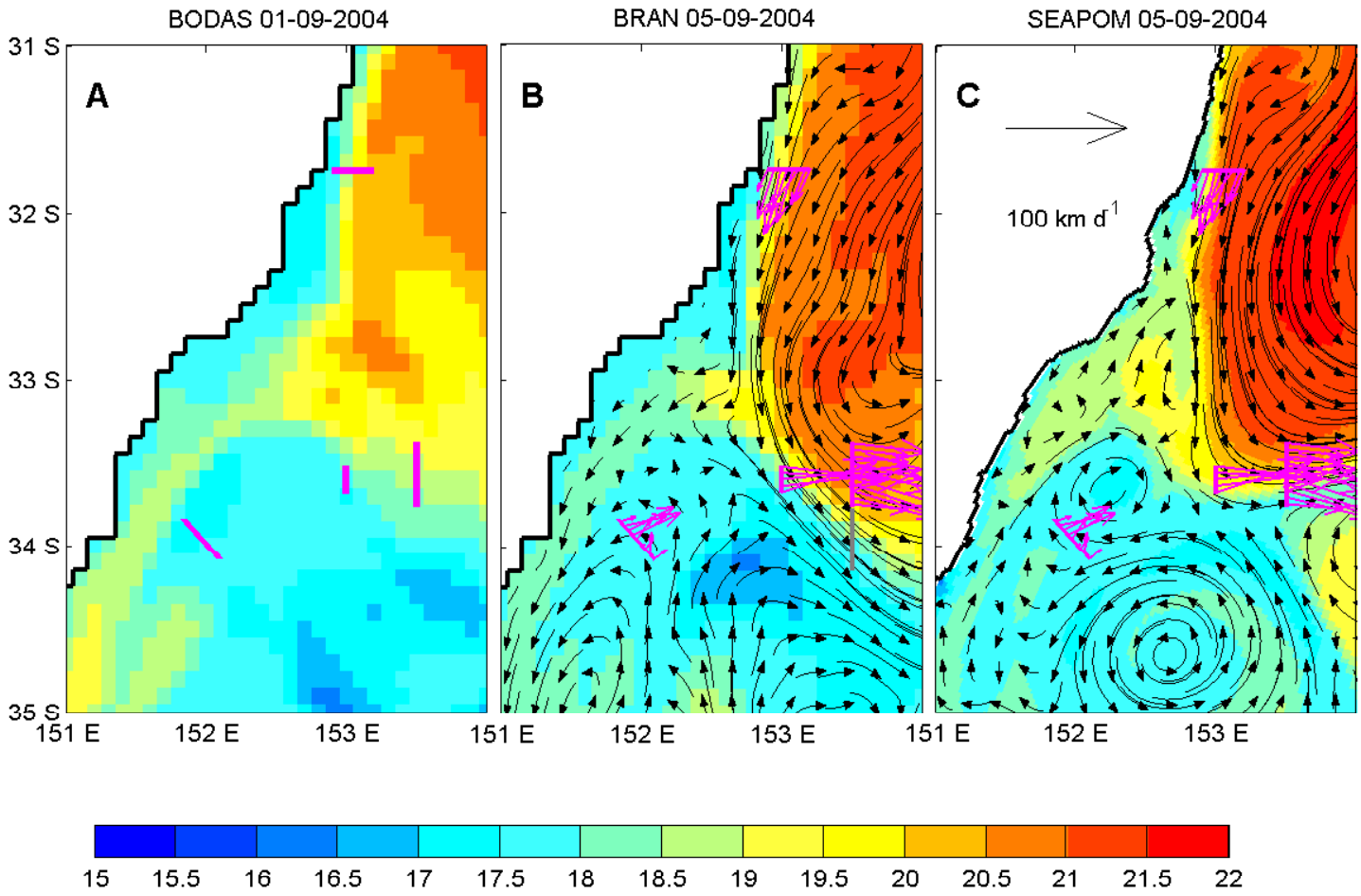
BODAS 01-09-2004
BRAN 05-09-2004
SEAPOM 05-09-2004
A
B
C
100 km d-1
31 S
32 S
33 S
34 S
35 S
151 E
152 E
153 E
15
15.5
16
16.5
17
17.5
18
18.5
19
19.5
20
20.5
21
21.5
22

Figure 6

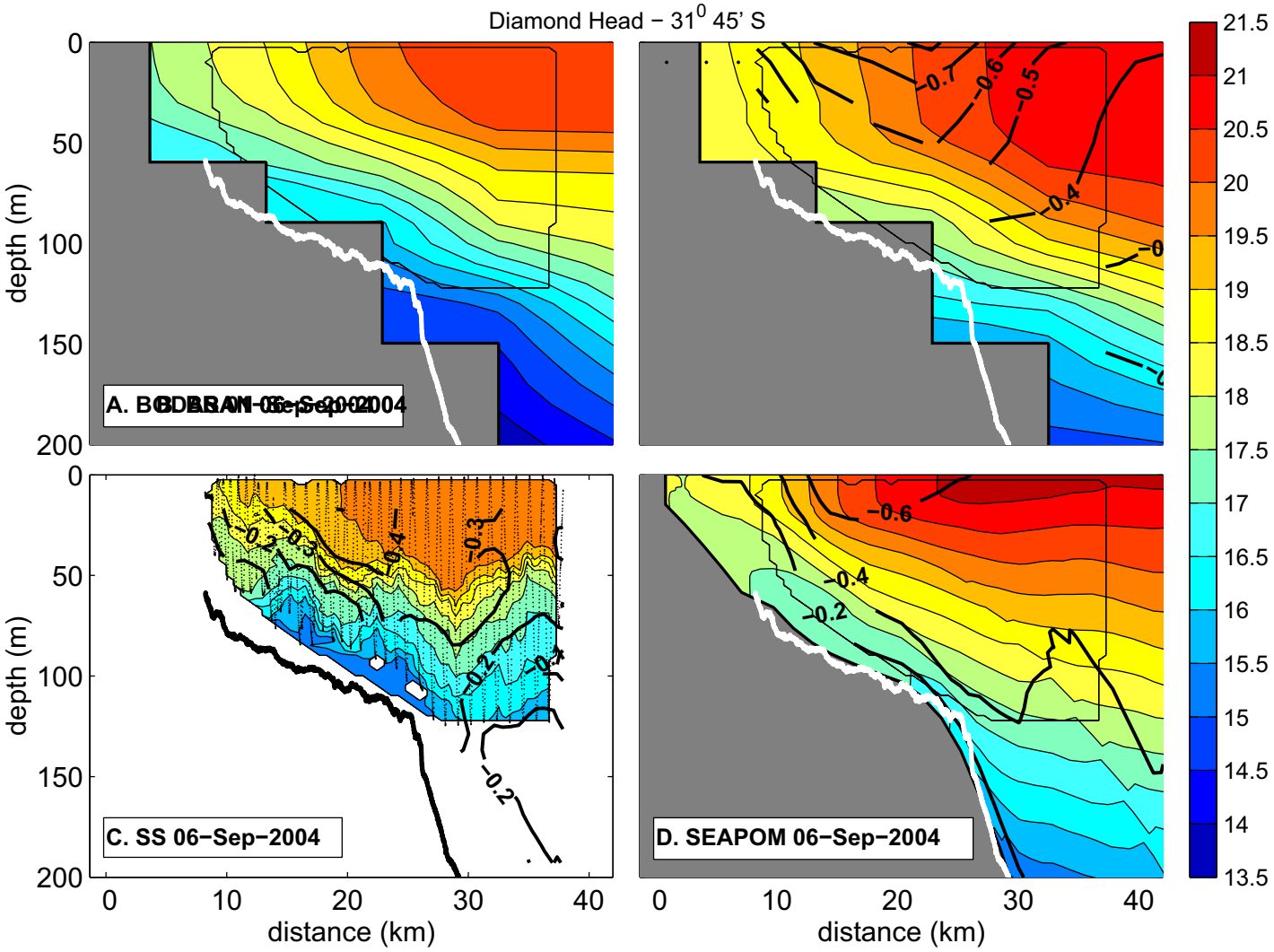
Diamond Head – 31^0 45' S
depth (m)
distance (km)
A. BODAS 06-Sep-2004
C. SS 06-Sep-2004
D. SEAPOM 06-Sep-2004
0
50
100
150
200
0
10
20
30
40
21.5
21
20.5
20
19.5
19
18.5
18
17.5
17
16.5
16
15.5
15
14.5
14
13.5

Figure 7

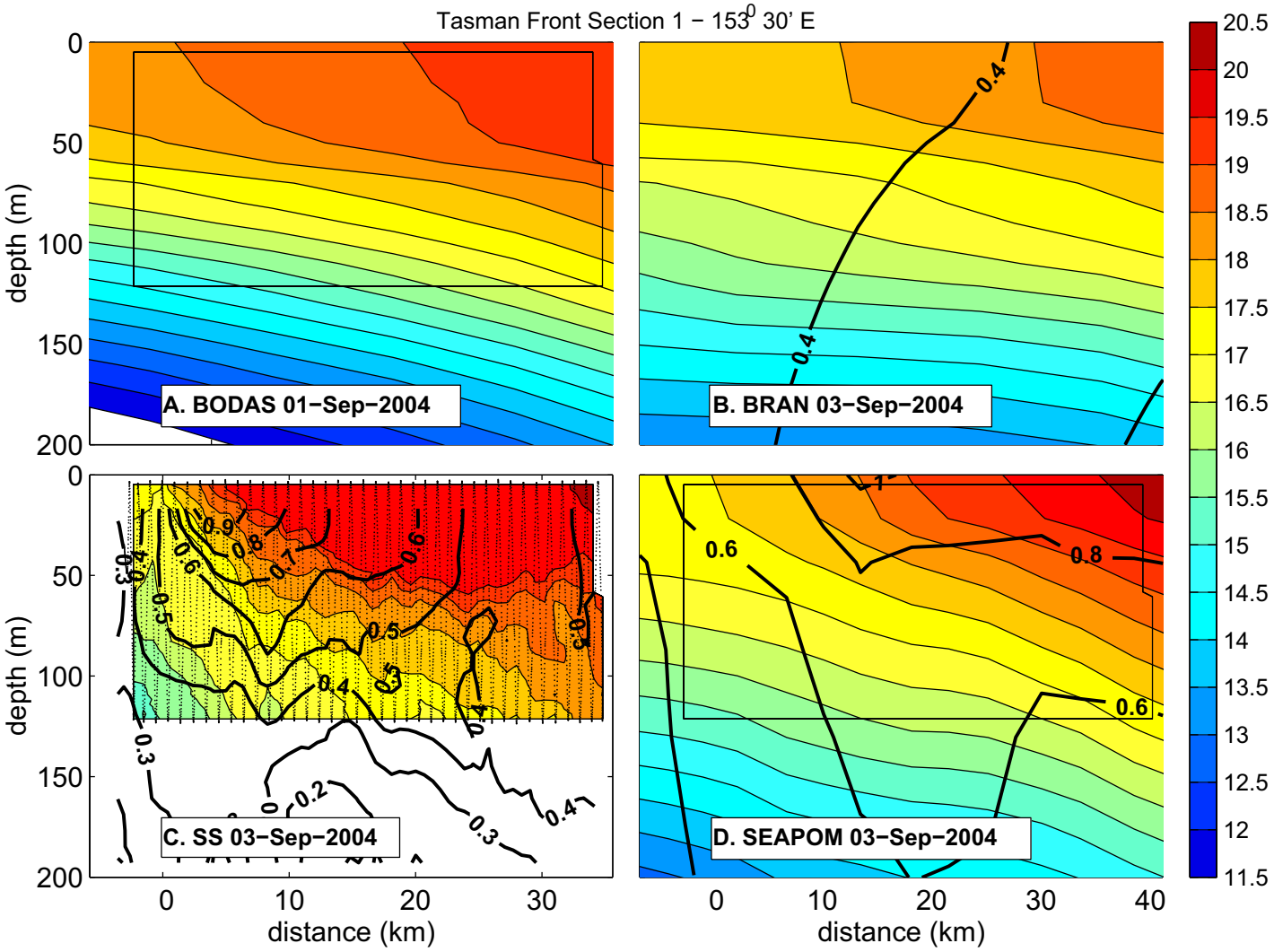
Tasman Front Section 1 − 153^0 30' E
A. BODAS 01−Sep−2004
B. BRAN 03−Sep−2004
C. SS 03−Sep−2004
D. SEAPOM 03−Sep−2004
depth (m)
distance (km)
0
50
100
150
200
10
20
30
40
20.5
20
19.5
19
18.5
18
17.5
17
16.5
16
15.5
15
14.5
14
13.5
13
12.5
12
11.5

Figure 8

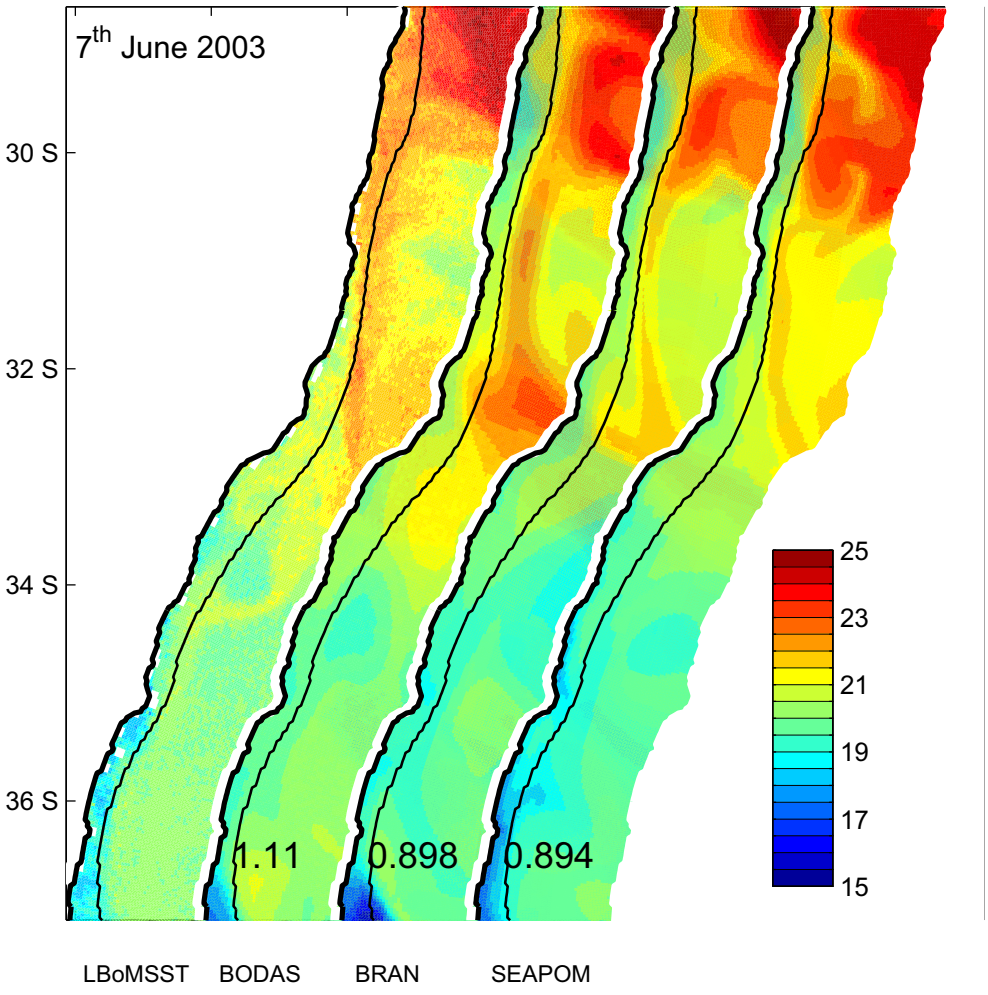
7th June 2003
30 S
32 S
34 S
36 S
1.11
0.898
0.894
25
23
21
19
17
15
LBoMSST
BODAS
BRAN
SEAPOM

Figure 9

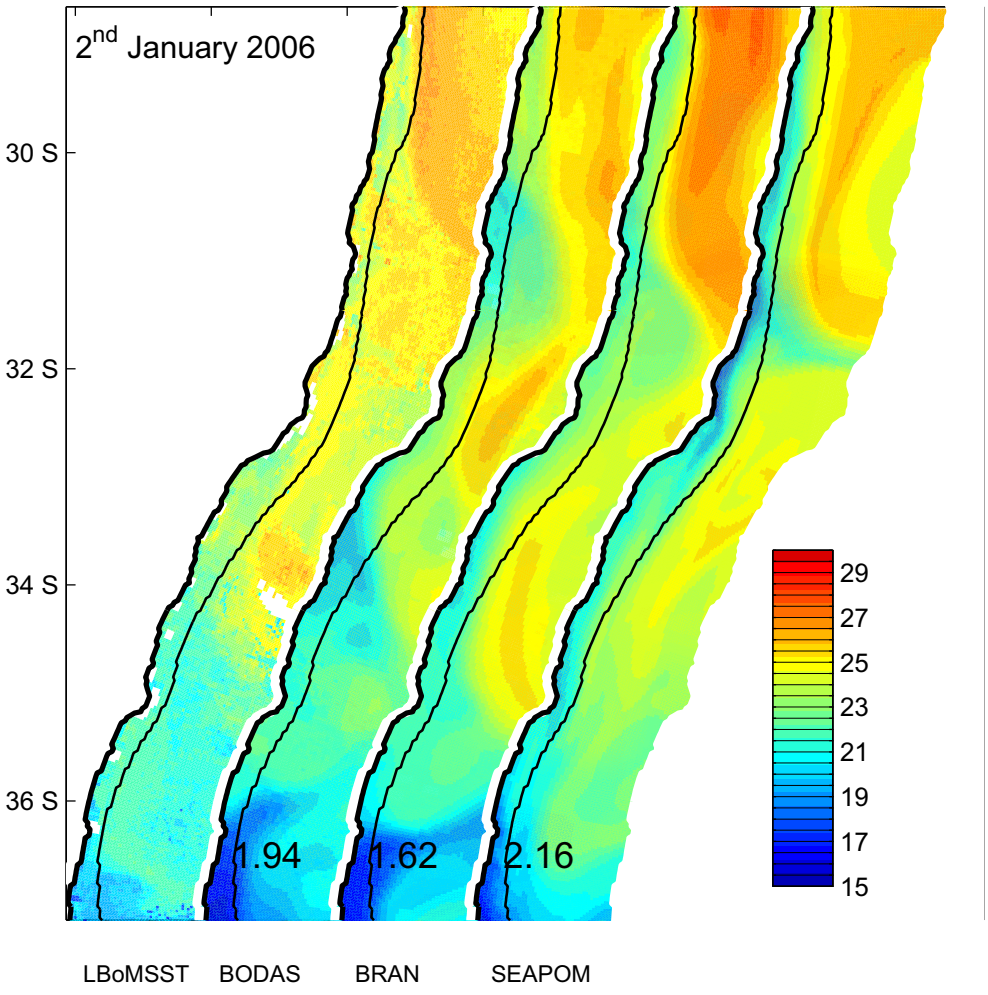
2nd January 2006
30 S
32 S
34 S
36 S
1.94
1.62
2.16
29
27
25
23
21
19
17
15
LBoMSST
BODAS
BRAN
SEAPOM

Figure 10

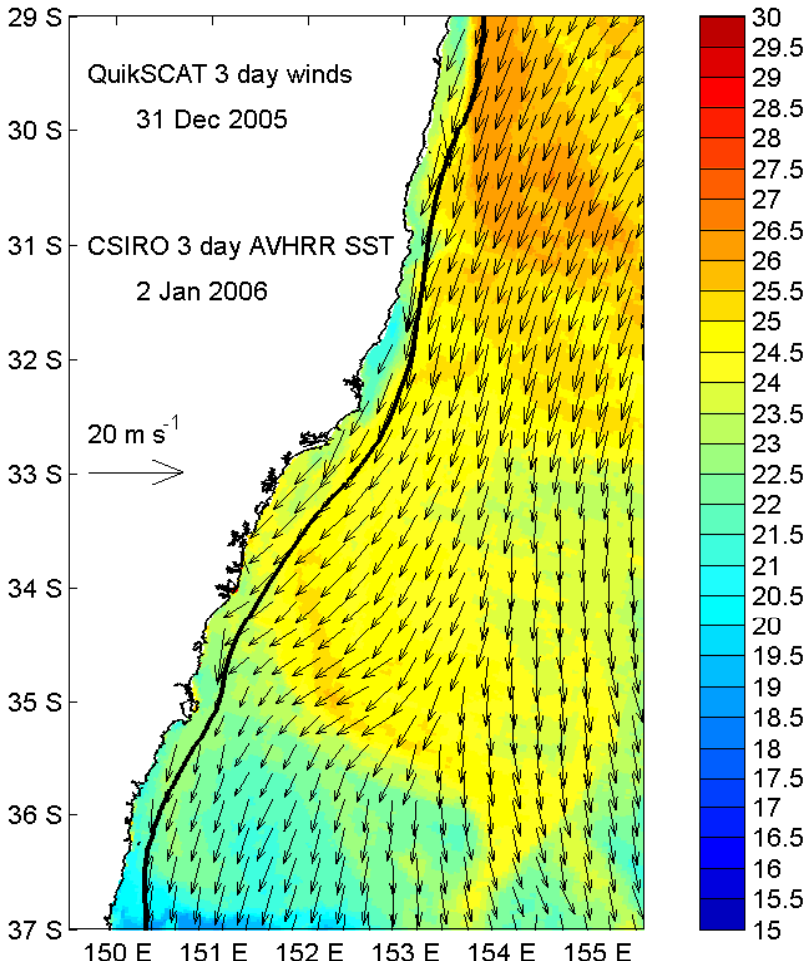
QuikSCAT 3 day winds
31 Dec 2005
CSIRO 3 day AVHRR SST
2 Jan 2006
20 m s-1
29 S
30 S
31 S
32 S
33 S
34 S
35 S
36 S
37 S
150 E
151 E
152 E
153 E
154 E
155 E
30
29.5
29
28.5
28
27.5
27
26.5
26
25.5
25
24.5
24
23.5
23
22.5
22
21.5
21
20.5
20
19.5
19
18.5
18
17.5
17
16.5
16
15.5
15

Figure 11

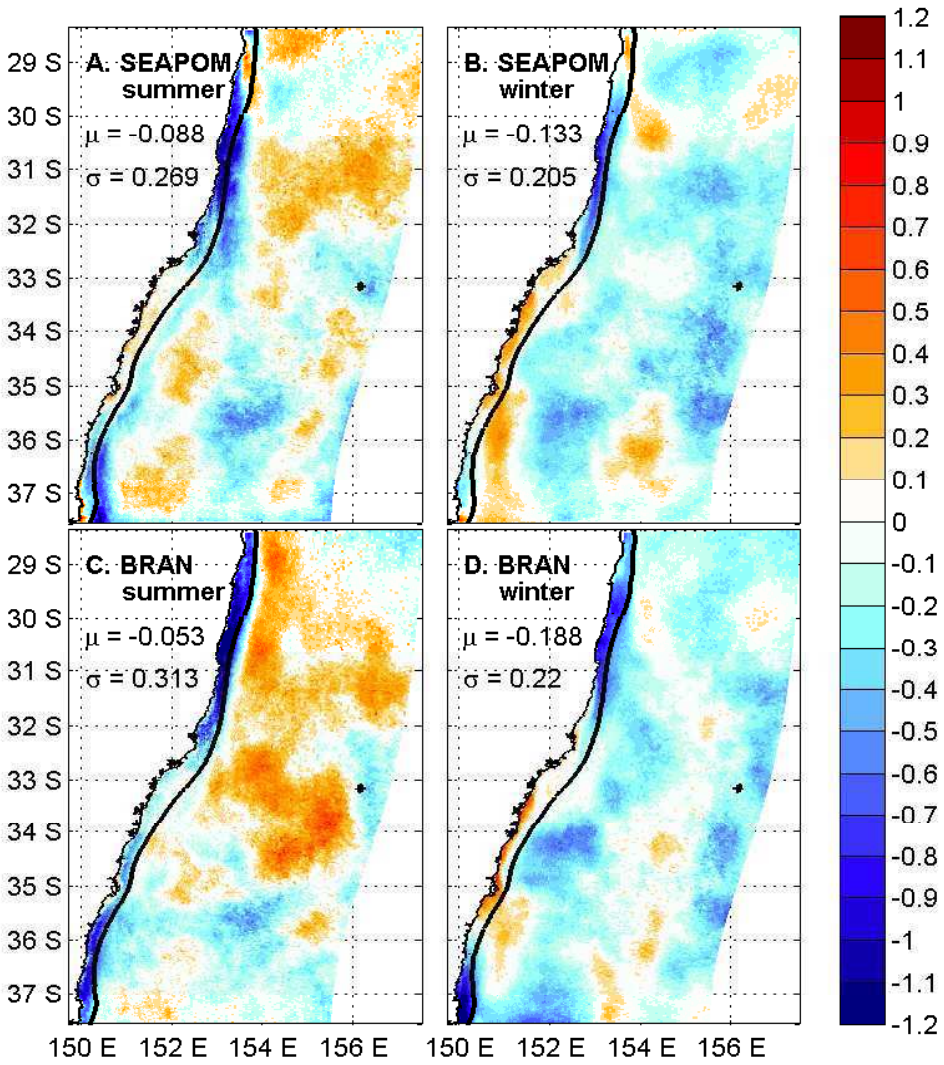
A. SEAPOM
summer
μ = -0.088
σ = 0.269
B. SEAPOM
winter
μ = -0.133
σ = 0.205
C. BRAN
summer
μ = -0.053
σ = 0.313
D. BRAN
winter
μ = -0.188
σ = 0.22
29 S
30 S
31 S
32 S
33 S
34 S
35 S
36 S
37 S
150 E
152 E
154 E
156 E
1.2
1.1
1
0.9
0.8
0.7
0.6
0.5
0.4
0.3
0.2
0.1
0
-0.1
-0.2
-0.3
-0.4
-0.5
-0.6
-0.7
-0.8
-0.9
-1
-1.1
-1.2

Figure 12

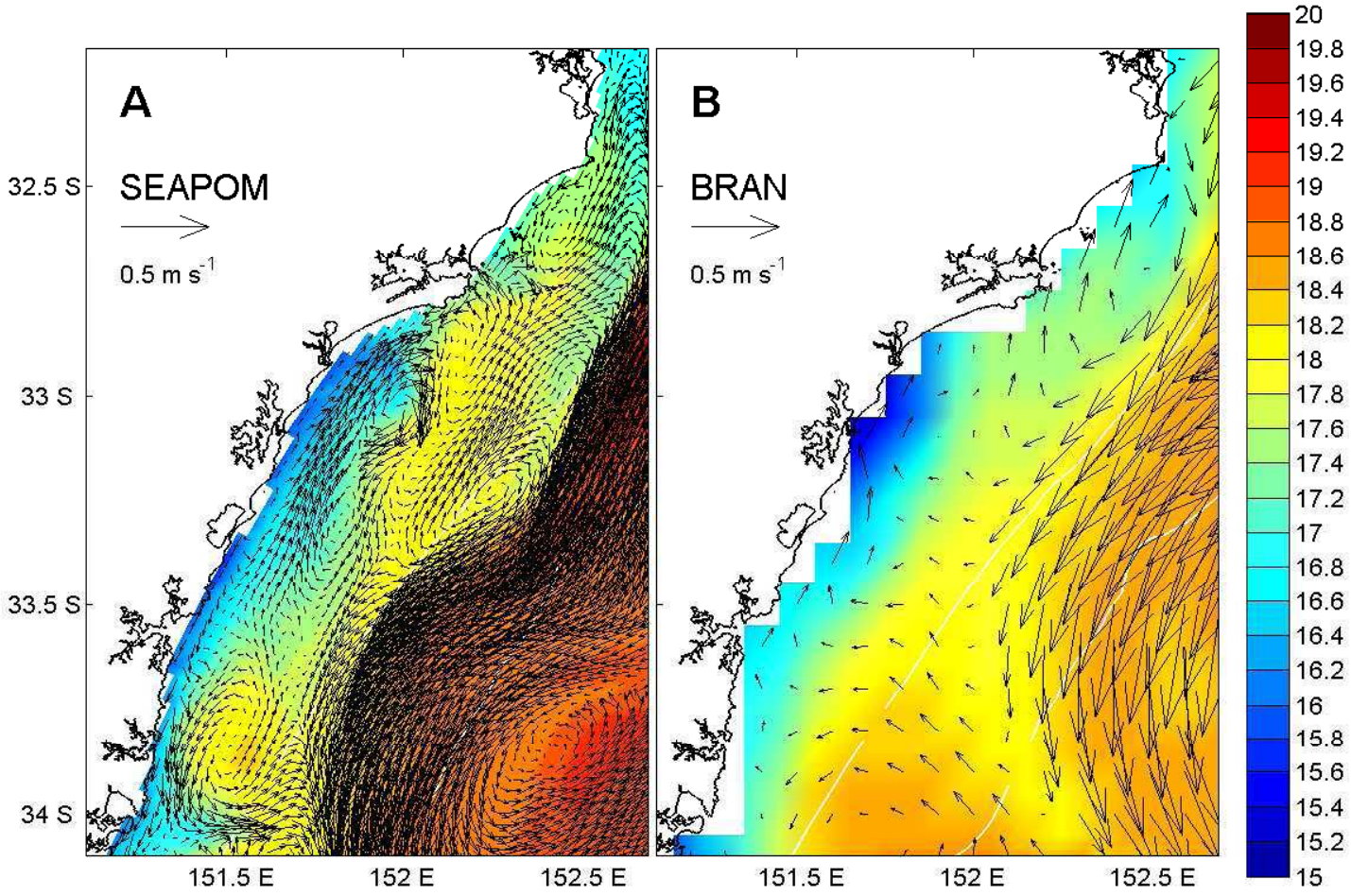
A
SEAPOM
0.5 m s-1
B
BRAN
0.5 m s-1
32.5 S
33 S
33.5 S
34 S
151.5 E
152 E
152.5 E
151.5 E
152 E
152.5 E
20
19.8
19.6
19.4
19.2
19
18.8
18.6
18.4
18.2
18
17.8
17.6
17.4
17.2
17
16.8
16.6
16.4
16.2
16
15.8
15.6
15.4
15.2
15